Proton beam writing a platform technology for high quality three-dimensional metal mold fabrication for nanofluidic applications

J. A. van Kan, P. G. Shao, Y. H. Wang & P. Malar

✎ Springer

TECHNICAL PAPER

Proton beam writing a platform technology for high quality three-dimensional metal mold fabrication for nanofluidic applications

J. A. van Kan · P. G. Shao · Y. H. Wang · P. Malar

Abstract Direct write nanolithographic techniques are powerful techniques to fabricate masters for nano-imprint lithography (NIL). Proton beam writing (PBW) is a relatively new technique which has shown great potential in fabricating three-dimensional (3D) nanostructures in polymer resist material down to the 20 nm level. MeV protons generate secondary electrons and like in many lithographic processes these electrons modify the molecular structure of the resist. The energies of the proton induced secondary electrons are relatively low compared with secondary electrons generated using electron beam writing, therefore proton induced secondary electrons only modify resist material within several nano meters of the proton track. Since protons mainly interact with the substrate electrons the path of the proton beam is very straight, resulting in smooth and well defined resist structures with practically no proximity effects. Further development of current proton beam technology, required to approach sub 10 nm structuring with MeV protons is discussed. To explore the full micro- and nano-fabricating capabilities of PBW it is important to investigate potential new resist materials. In PBW mass production can be achieved through the fabrication of reliable molds and stamps. The compatibility of MeV proton beams for resist materials and post processing steps like electroplating and resist removal are evaluated. The second focus of this paper is PDMS nanofluidic lab on a chip sorting devices using high quality Ni molds. These molds have been prepared via PBW and Ni electroplating, a release layer on a Ni mold allows fine feature replication down to the 300 nm level with high aspect ratios in PDMS.

J. A. van Kan (✉) · P. G. Shao · Y. H. Wang · P. Malar
Department of Physics, CIBA, NUS,
117542 Singapore, Singapore
e-mail: phyjavk@nus.edu.sg

1 Introduction

Commonly used lithographic techniques are essentially two-dimensional (2D) and are very successful in micro-electromechanical systems (MEMS) and nano-electromechanical systems (NEMS). High aspect ratio 3D microstructures with nanometer details are of growing interest. Typical applications can be found in lab on a chip fluidic devices or optoelectronic devices. In recent years, microfluidic systems have become an important platform for biological and chemical research (Yager et al. 2006; Ottesen et al. 2006). The complexity of microfluidic systems is increasing rapidly (Thorsen el al. 2002) and new ways of detecting and investigating biological cells and molecules with higher sensitivity are being developed (Phillips and Cheng 2005), nonetheless the field is still at an early stage of development (Whitesides 2006).

Contamination prohibits the re-usage of fluidic chip devices, making a reproducible high throughput fabrication technique important for the successful development of micro/nano fluidic systems. A very promising technique to meet the required throughput and accuracy is nano-imprint lithography (NIL). Consequently, polymer instead of silicon or quartz is often considered as a better choice for making microfluidic devices (Song and Lee 2006). Several groups have been using PDMS and other polymers to fabricate micro and nanofluidic channels (Lei Zhang et al. 2008; Xianqiao Hu et al. 2011), often nanometer dimensions are obtained but accurate shape control at the sub micron level is not easy to achieve. Other groups have used alternative materials to replicate nanofluidic channels (Rolland et al. 2004; De Marco et al. 2008).

In scaling fluidic chips down to the nano level with high aspect ratios it is beneficial to develop new nanolithographic techniques. In the centre for ion beam applications

(CIBA), national university of singapore (NUS) we have developed proton beam writing (PBW) and shown it can potentially provide high quality 3D nanostructures (van Kan et al. 2003a; Chin 2003). In PBW a MeV proton beam is focused down and scanned across a resist material. In this energy regime protons will mainly interact with substrate electrons, coupled with the mass mismatch between protons and electrons the protons will lose their energy in many small discreet steps. SRIM (Biersack and Haggmark 1980) calculations show that this leads to a beam spread of only a few nano meters, the exact value depends on beam energy and substrate material (van Kan et al. 2000). When calculating the energy deposition due to the proton induced secondary electrons (Udalagama et al. 2009) it is clear that PBW has the potential to make structures below 10 nm in width in layers of at least 500 nm in thickness.

To achieve features below 10 nm using PBW several technological challenges need to be met. We have identified three main challenges; Firstly the capability to focus MeV proton beams. With the introduction of a new focusing system (Watt et al. 2011; van Kan et al. 2011) proton beams can now regularly be focused down to 30 nm beam spot sizes. This new lens system is undergoing further optimization and smaller beam spot sizes are expected in the near future.

Secondly the proton source brightness in available PBW systems (Watt et al. 2003; Szymanski and Jamieson 1997) is typically six orders of magnitude weaker compared to state of the art electron sources (Swanson and Schwind 2008) or focused ion beam (FIB) sources (Hagen et al. 2008).

Thirdly a suitable resist material and development procedure (Bolhuis et al. 2009) needs to be employed to render the energy deposition profile of the protons in usable nanostructures. In this paper we will discuss recent achievements in these areas and an outlook on what needs to be done to achieve PBW below 10 nm.

The major focus of this paper will be on the fabrication of high quality Ni molds obtained using PBW. These Ni molds feature high aspect ratios with details down to 300 nm. A special release layer is tested to enhance the performance of these Ni molds in PDMS soft lithography. To demonstrate the potential of these Ni molds examples of nanofluidic ratchet chips are discussed.

2 PBW facility design considerations and performance

In the CIBA at the NUS five state of the art beamlines are installed, see Fig. 1. At 10° with respect to the switcher magnet focused MeV proton beams have been utilized in different areas of research such as PBW, imaging of biomedical samples, silicon micromachining and photonics (Watt et al. 2005).

PBW is a new direct-writing technique that uses a focused beam of MeV protons to pattern resist material at nanodimensions (Watt et al. 2007). PBW has two fundamental advantages over electron beam writing: firstly proximity effects are greatly reduced (Whitlow et al. 2004; Udalagama et al. 2007), which allows the fabrication of high-density high aspect ratio nanostructures, and secondly PBW has typically a 100-fold higher sensitivity compared with electron beam writing in the same resist material (van Kan et al. 2007). CIBA holds the world record for focusing protons down to 35×75 nm^2 (Watt et al. 2003) and have produced 3D high aspect ratio walls down to 22 nm in hydrogen silsesquioxane (HSQ) (van Kan et al. 2006). The PBW results presented in this paper were obtained utilizing the 10° beamline, more details about this beamline were reported earlier (van Kan et al. 2003a, b).

The rapid growth in nanotechnology coupled with the difficulties in 3D nanofabrication has fuelled the quest for further downsize in beam spot size. This requires improvement to the focusing capabilities of the existing system and places stringent conditions on the control of aberrations and other parameters. For this purpose a new dedicated PBW test line has been constructed at 20° to study the effectiveness of several factors like sensitivity of the focusing system to external stray fields, quadrupole lens power supplies with improved stability and slit design. This system features a high demagnification lens system based on compact OM52 lenses with reduced working distance. The system will be tested in a variety of high demagnification configurations including the spaced Oxford triplet and the double crossover Russian quadruplet. It features an electrostatic scanning system and a new collimator slit aperture design. Preliminary results on beam focusing show that the new beamline is capable of focusing beams down to 20 nm dimensions utilizing a spaced Oxford triplet configuration (van Kan et al. 2011). In future we will also test the Russian quadruplet in spaced double-crossover mode, which has greatly increased demagnifications in both the X and Y directions (Grime and Watt 1984).

The currently available proton sources used in MeV systems have relatively low brightness (Watt et al. 2003; Szymanski and Jamieson 1997). The most successful source is an RF ion source based on a 60-year-old design (Moak et al. 1951). To further optimize the performance of the new PBW system in CIBA research is planned to test and develop high brightness ion sources.

3 Resist materials for PBW

To expand the applications of PBW in NIL it is important to investigate potential new resist materials, re-evaluate currently available resist materials and test the suitability of

Fig. 1 Schematic layout of the CIBA accelerator facility. The new proton beam writing line is installed at 20° with respect to the switcher magnet. In the photograph the new PBW line and the original 10° PBW line are visible
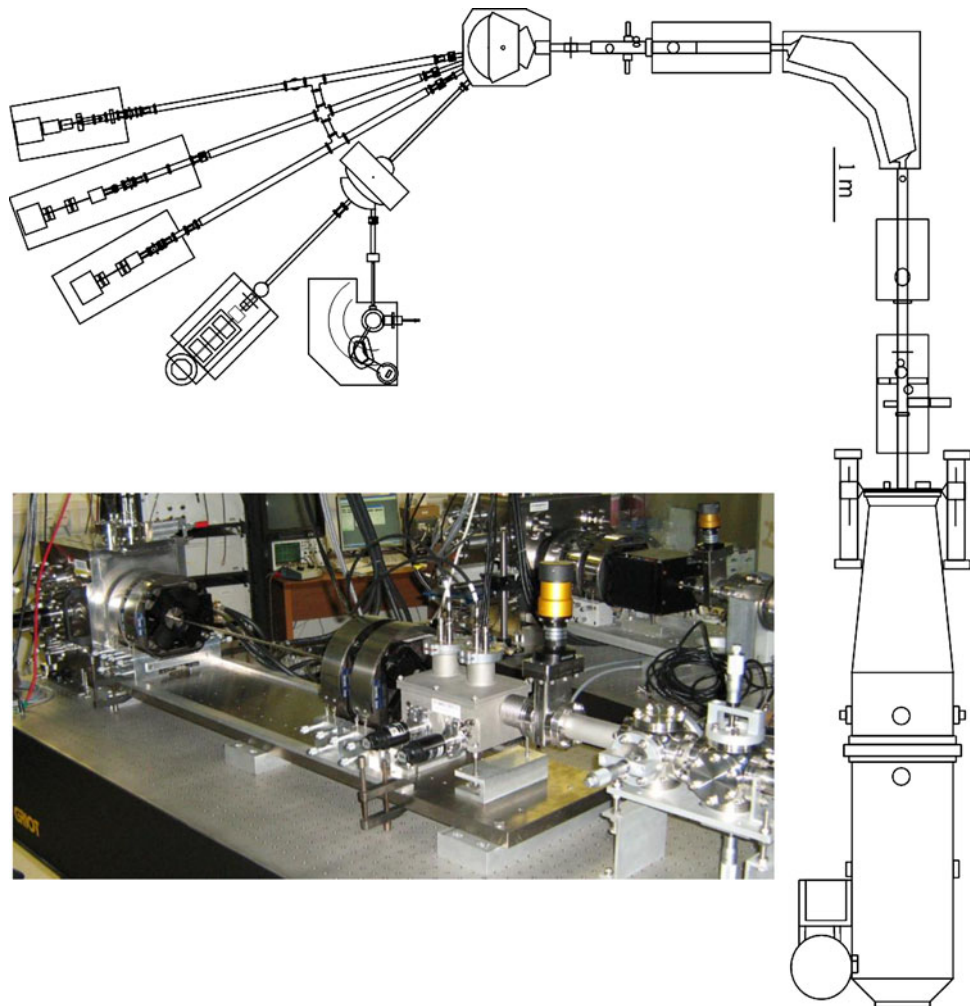

resist materials for mold fabrication. PMMA, SU-8 and HSQ have demonstrated sub 60 nm lateral details featuring high aspect ratios (van Kan et al. 2003a, 2006). Here we introduce AR-P 3250 (ALLRESIST GmbH) as potential new resist material for PBW and compare this to ma-P 1275HV (Micro Resist Technology GmbH) (Liu et al. 2010). Ma-N series and WL-7154 resist will be re-evaluated. Typically PBW shows similar resist contrast compared with electron beam writing on the same resist materials (Bolhuis et al. 2009).

In PBW a resist can be used for different purposes. Firstly protons can be used to prototype nanostructures directly into resist. Secondly a resist can be used as a mold for replication of micro- and nano-structures. Soft lithography (Chabinyc et al. 2001) is a nice example where PDMS fluidic lab on chip devices can be easily obtained. In CIBA polymer molds fabricated using PBW are regularly used to fabricate nanofluidic lab on chip devices for single molecule DNA studies (Zhang et al. 2009, 2008). Resist masters can also be used as a template for the fabrication of nanowires at desired locations, as precise components in

integrated devices, these nanowire structures could in future be integrated into optofluidic devices (Erickson et al. 2008). To fabricate more durable molds a resist mold can be used as a template to form a Ni mold through a Ni electroplating process. The hard Ni mold can then be used in NIL replication like injection molding, PDMS soft lithography and nanoimprinting. Therefore different applications have different resist requirements. Next we will present data on new resist materials for PBW and evaluate their potential applications in combination with PBW.

AR-P 3250 resist is a positive resist under i-line (365 nm) exposure. It is designed for layer thickness of about 4–40 μm. To test the compatibility with PBW a $\sim$5 μm thick layer was spin coated on an Au/Cr coated Si wafer. First the wafer was dry baked at 200°C to remove any moist, next the wafer was coated at 4000 rpm for 30 s, followed by a bake at 95°C for 12 min to completely remove the solvent. Initial PBW tests on this resist were performed with exposure doses ranging from 20 to 100 nC/mm², comparable to other PBW resist materials. In
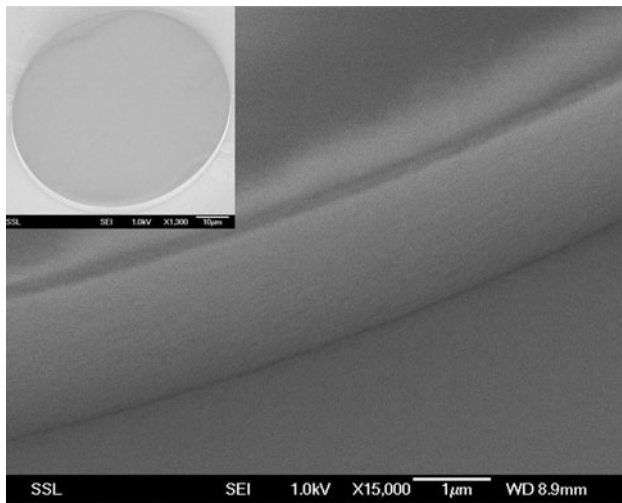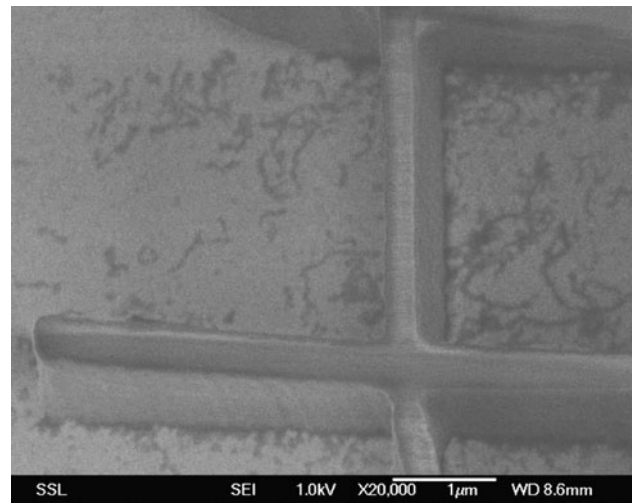
Fig. 2 High magnification SEM photo of the AR-P 3250 resist after PBW (60 nC/mm2) and flood UV exposure, featuring a smooth sidewall profile, the inset shows an overview of the whole pillar

Fig. 3 High magnification SEM photo of the WL-7154 resist after PBW using 1 MeV protons and a dose of 8 nC/mm2

this test 60 μm diameter circles were exposed. After development no clear structures were obtained. Next we decided to perform a flood UV exposure on the film followed by development in AR 300-26 developer (1:1 diluted with DI water) for 1 min. As can be observed in Fig. 2 the resist crosslinks under proton exposure and the surrounding resist is removed during development after the flood UV exposure. As can be seen smooth and vertical sidewalls are observed. Like ma-P 1275HV resist the AR-P 3250 resist preferentially undergoes cross linking under proton beam exposure (Liu et al. 2010). The minimum proton dose required for successful structuring of the AR-P 3250 is 40 nC/mm^2.

In future experiments more tests on AR-P 3250 in combination with PBW and UV lithography will be performed. Using this approach large feeding channels can be fabricated with UV lithography whereas critical features with vertical side-walls in fluidic channels will be fabricated using PBW. To convert the AR-P 3250 into a Ni mold experiments are planned to electroplate this resist polymer. AR-P 3250 is therefore a potential candidate to either generate resist molds or possibly Ni molds for soft-lithography and NIL applications.

WL-7154 from Dow Corning is a photo-patternable spin-on silicone. This resist can be patterned using i-line lithography. This resist can be applied in layers up to several microns. WL-7154 is a negative tone resist under proton beam exposure and shows high sensitivity for protons (4 nC/mm^2). Here a layer was spun at 1,500 rpm for 30 s to yield a thickness of 1.4 μm. After exposure the structures are developed in mesitylene for 60 s. It was found to be beneficial to rinse the sample in DI water followed by a short rinse in fresh developer and again a rinse in DI water.

To test the production of small feature sizes in WL-7154 using PBW we exposed a 1.4 μm thick layer of WL-7154 resist by writing a grid pattern, digitized in a matrix of $4,096 \times 4,096$ pixels in a scan area of 100×100 μm^2. In order to achieve smooth side walls the pixel size was chosen smaller than the beam size. A 1 MeV proton beam was focused down to 60×90 nm^2, as measured using a resolution standard made by Zhang et al. (Zhang et al. 2007), and a dose of 8 nC/mm^2 was used in this experiment. Next the sample was developed as described above using a second rinse step with fresh developer. The lines obtained are shown in Fig. 3. The lines are only about 260 nm in width in x direction closely matching the expected size. These lines exhibit an aspect ratio of more than 5. In this experiment the applied dose was only twice the minimum dose for cross-linking rendering the lines relatively weak.

WL-7154 shows promise for high aspect ratio nano fabrication but due to its high sensitivity, any scattered beam will give rise to a thin residual layer of resist on the Si substrate, see Fig. 3. Therefore proton structuring and development of WL-7154 requires more fine tuning before it can be effectively used in PBW applications.

MaN-2400 (Micro Resist Technology GmbH) is a negative tone photoresist series designed for the use in micro- and nano-electronics. The maN-2400 series is a DUV sensitive negative tone resist that is composed of a phenolic resin (Novolak) as polymeric binder and a bisazide as photoactive compound (PAC) (Bilderan et al. 2009). Menzel et al. have shown Ni grids faithfully replicated from PBW fabricated maN-440 resist structures (Menzel et al. 2007). Here we introduce maN-2410 in combination with PBW, according to the supplier this resist is able to support finer details in combination with electron beam writing compared to maN-440 (Private Communication).

In processing maN-2410 a layer of Au/Cr is deposited using magnetron sputtering onto two Si wafers, then these wafers are dry baked at 200°C to remove any moist. Next the two wafers are spin coated to yield thicknesses of 600 nm and 1 μm. The maN-2410 layers are exposed using a 1 MeV proton beam focused down to a spot size of 100×120 nm^2 using a dose ranging from 70 to 200 nC/mm^2. After PBW the samples are developed in ma-D 525 for 130–150 s, rinsed with DI water for 2–3 min and air dried. To guarantee a smooth formation of a Ni stamp during the electroplating process a 6 nm Ti layer is coated onto the sample as a secondary seed layer before the Ni electroplating. Electroplating is performed in a Technotrans RD 50 plating machine, the first 10 μm is plated slowly at a rate of 52 A/dm^2 then the rate is increased to 520 A/dm2 for 41.5 h, yielding a total thickness of 2.5 mm.

As can be seen in Fig. 4a lines in maN-2410 can be written down to 250 nm in width in the 600 nm thick sample, this is about a factor of 2 smaller than reported earlier (Menzel et al. 2007). In Fig. 4b we see lines ranging from 500 to 1,000 nm in width in the 1 μm thick sample. As can be seen in Fig. 4c the lines were transferred from the maN-2410 resist pattern to the Ni mold accurately and the resist was removed easily with acetone. SU-8 patterned negative tone resist on the other hand is very difficult to be removed from the electroplated metal replica. This is a major obstacle in the fabrication of metal molds with details down to the micro- and nano-scale, especially when the aspect ratio of the pattern is high. These results indicate that patterning maN-2410 resist with PBW is promising process for making high quality Ni molds with high aspect ratio featuring details at the micro- and nano-scale.

4 Ni molds for PDMS fabrication of nm details

There are basically two types of molds that can be produced in PBW; Polymer molds or metallic molds. In this section we will discuss the fabrication of high quality Ni molds used in PDMS nanofluidic lab on chip replication.

A wide variety of PDMS fluidic chips, have been developed which provide an important platform for biological research such as DNA analysis (Yea et al. 2006). PDMS has also distinguished itself with material property advantages e.g. a wide compatibility with biological materials, its transparency offers easy observation and optical signal detection. Many researchers enjoy the convenience of fabricating PDMS fluidic systems with feature dimensions of a few tens of micrometers, advanced systems sometimes have details in the range of 1–10 μm.

Fabrication of fluidic structures with sub-micro and nano feature dimension is important because interaction of such structures is used to manipulate large molecules like
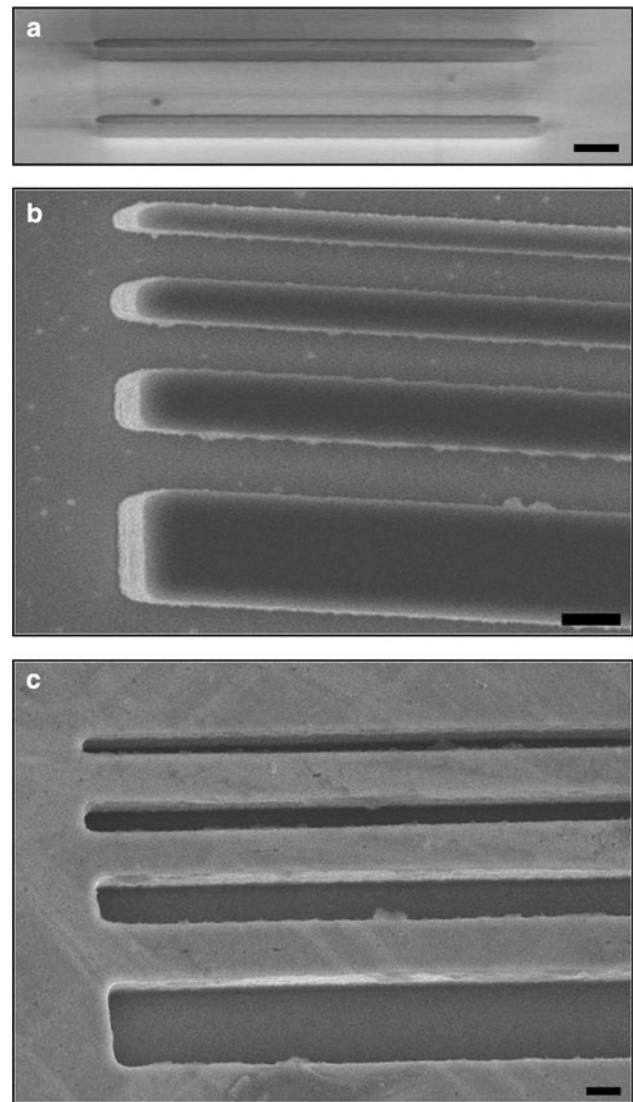
Fig. 4 **a** SEM image of 250 nm wide lines in a 600 nm thick maN-2410 resist layer written with a 1 MeV proton beam. **b** SEM image of 1 μm thick maN-2410 resist lines written with a 1 MeV proton beam featuring lines down to 500 nm in width. **c** SEM image of Ni electroplated mold from **b**, featuring grooves down to 500 nm in width and 1 μm deep. All scale bars are 1 μm long

DNA in a fluidic environment. For complicated geometries and smaller sizes it is difficult to replicate lab on chip devices in PDMS. The main limitation in achieving smaller feature sizes with relatively high aspect ratios in PDMS replication can be attributed to the poor quality of the molds available. Realizing complicated arrays for DNA molecular sorting devices, researchers have turned to silicon or quartz devices fabricated by electron beam writing and reactive ion etching (RIE) (Huang et al. 2004). These techniques can produce very small feature sizes in lab on chip devices. The downside is the relatively low yield and the fact that these techniques are not as easily available as PDMS replication. The mechanical strength of the template

material is critical for PDMS replication, especially when the feature dimensions are in the nanometer regime featuring high aspect ratios. In a template made of PMMA or other resist material features in the nano-regime can easily deform and or delaminate from the substrate. During replication, the template will get contaminated and therefore needs to be cleaned with chemical solvents and ultrasonic agitations which will damage photoresist templates. For successful PDMS replication templates of high strength are therefore vital. Hard Ni molds have the added advantage that they can be easily cleaned compared to polymer molds. Here we demonstrate the power of PBW through high quality Ni mold fabrication and PDMS casting. The PBW fabricated Ni molds can in future also be used employing other NIL techniques or alternative polymer materials for replication following the process described by Rolland et al. 2004 and De Marco et al. 2008.

Since PBW has proven to be a powerful technique for the production of metallic molds (Ansari et al. 2004), Ni templates are evaluated for the PDMS replication process fabricating ratcheted arrays with feature sizes in the nanometer regime. In literature people have discussed different ratchet chip designs (Cisne et al. 2011). The design we chose for our first lab on chip design is based on a theoretical idea for DNA separation using Brownian motion in lab on chip devices (Ertas 1998).

As shown in Fig. 5a, a 2 μm thick Ni mold featuring the ratcheted fluidic chip was successfully electroplated from a proton beam written PMMA structure. Directly replicating PDMS layers from this Ni mold was not successful. The geometry of the ratcheted structure has sharp angles which are nucleation sites for crack formation during de-molding.

Teflon AF® 1600 is a commercial amorphous copolymers of polytetrafluoroethylene (PTFE) with 2, 2-bis(triflouromethyl)-4,5-difluoro-1, 3-dioxole developed by DuPont in 1990s. In addition to retaining PTFE properties, the Teflon AF polymer has limited solubility in some commercially available perfluorinated solvents enabling it to be solution cast or spin coated into clear micron thin films (Makohliso et al. 1998).

Here Teflon AF 1600 is dissolved in FC-40. Since FC-40 has a relatively low vapor pressure (432 Pascal) it permits degassing under vacuum condition after spin coating, guaranteeing uniform coating of the Ni mold. Spincoating Teflon AF 1600 (0.02% in FC-40) on the Ni mold results in a 5 nm thick Teflon film. This thin Teflon film considerably promotes the release capabilities of the PDMS replica from the Ni mold. PDMS was cast on the Teflon coated Ni stamp, and cured at 60°C for 4 h. After releasing from the stamp, holes were punched in the PDMS replica which serve as fluidic reservoirs. As can be seen in Fig. 5b the 2 μm tall PDMS obstacles are well formed featuring sharp tips of 300 nm in width, this corresponds to
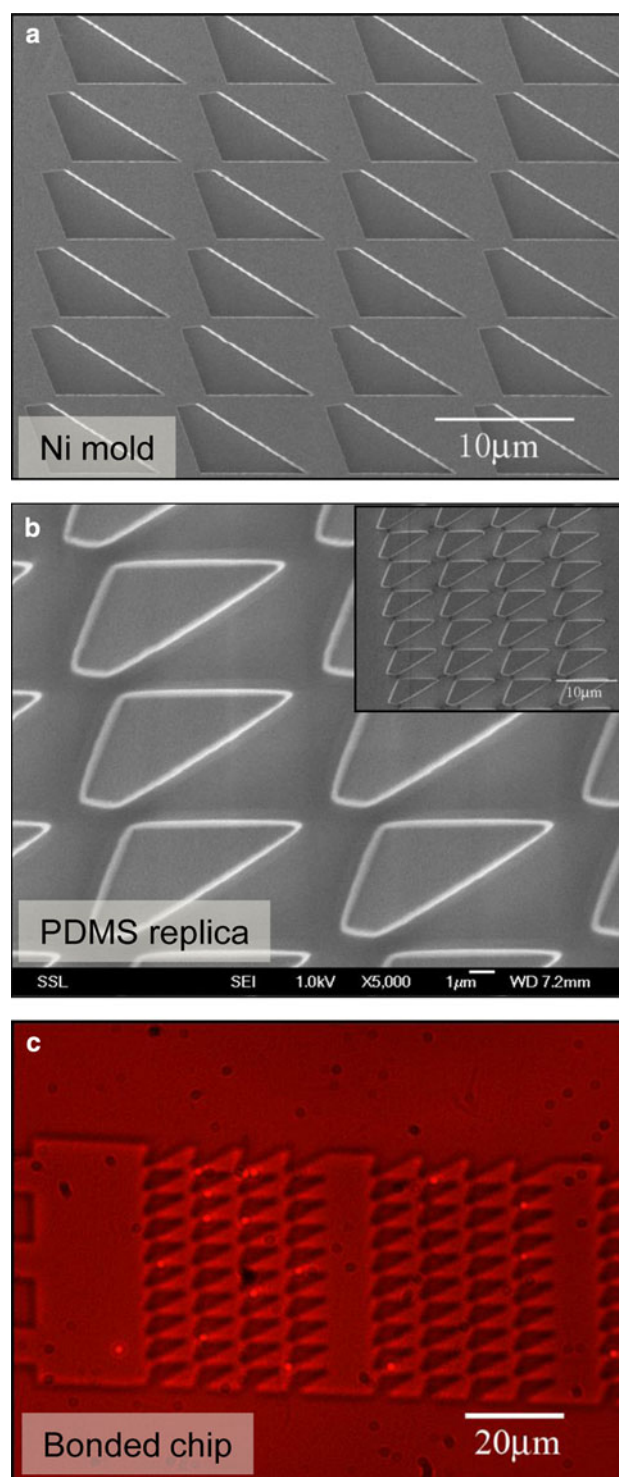
Fig. 5 a Ni template fabricated using PBW in PMMA followed by Ni electroplating, b PDMS replicated fine features, here the Ni was coated with a Teflon release layer. c Bonded PDMS fluidic chip with fluorescent nano spheres

an aspect ratio of more than 6. Next a quartz cover slip and the PDMS layer are treated with air plasma in a Harrick Plasma cleaner (250 mTorr for 15 s). Then the PDMS layer
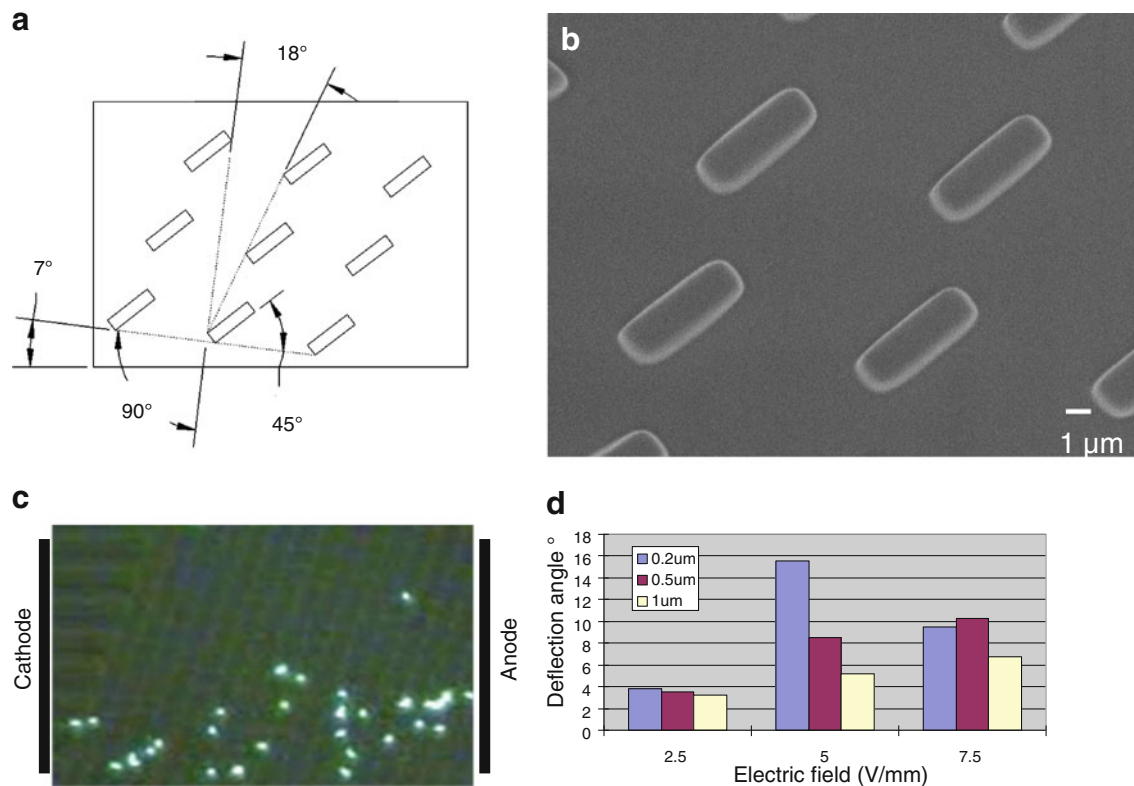
Fig. 6 **a** Detailed geometry of the Brownian ratchet chip, **b** PDMS Brownian structure replicated from the Ni master fabricated via PBW and Ni electroplating. **c** Chip test imaging 0.5 μm fluorescent nanospheres. **d** Deflection angles of fluorescent spheres of different sizes under different field strengths

is bonded onto the quartz substrate and an enclosed fluidic chip is obtained. As can be seen in Fig. 5c buffer solution with fluorescent spheres can be driven through this chip. Here we demonstrated successful replication of high aspect ratio PDMS nanostructure details in a PDMS fluidic chip device.

To achieve particle separation an adjusted design was used, this design features smaller obstacle structures and larger distances between the obstacle structures (Huang et al. 2003). A basic layout of the design is shown in Fig. 6a. The fabrication procedure for this design is the same as discussed for the earlier ratchet design. The replicated PDMS obstacles are again of high quality (see Fig. 6b). The replicated PDMS ratcheted structure is bonded to a quartz cover slip to establish an enclosed fluidic chip (see Fig. 6c). The chip is now ready for fluidic experiments with buffer solution containing fluorescent spheres. An electric field across the chip is applied through platinum electrodes at the cathode and anode, at the inlet and outlet of the fluid chip respectively. As shown in Fig. 6c, spheres of 500 nm flow from left to right through this chip driven by electrophoresis. Spheres diffusing down are blocked and deflected back to the original gap, whereas those diffusing up are deflected to the next gap on top. The movement of the

spheres is recorded and tracked with a MATLAB code. Different types of spheres are tested and the deflection angles for 250, 500 and 1,000 nm spheres are summarized in Fig. 6d. Typical error in the obtained angle is about 5%.

5 Conclusions

PBW is technically underdeveloped compared with electron beam writing and FIB technology. In spite of this the current system available at CIBA at the NUS is now capable of writing high aspect ratio structures down to the 20 nm level in resist material. The structures produced have smooth and vertical sidewalls, without observed proximity effects. Because of its minimal proximity effects, PBW has the capability of producing structures of high packing density. AR-P 3250 is introduced as a promising new resist material for PBW featuring smooth sidewalls. The performance of WL-7154 and maN-2410 resist have been improved and the minimum feature size for both is now 250 nm.

Since PMMA is still one of the highest resolution resist for PBW it was used in combination with electroplating to generate high quality molds for the replication of PDMS

nanofluidic chips. The lifespan of the Ni mold can be extended and the functionality improved by means of introducing a 5 nm thick Teflon AF release layer. This allows the replication of 300 nm details in PDMS fluidic lab on chip devices, featuring an aspect ratio of 6.

References

Ansari K, van Kan JA, Bettiol AA, Watt F (2004) Fabrication of high aspect ratio 100 nm metallic stamps for nanoimprint lithography using proton beam writing. Appl Phys Lett 85:476–478

Biersack J, Haggmark LG (1980) A monte carlo computer program for the transport of energetic ions in amorphous targets. Nucl Instrum Method 174:257–269

Blideran MM, Häffner M, Schuster B-E, Raisch C, Weigand H, Fleischer M, Peisert H, Chassé T, Kern DP (2009) Improving etch selectivity and stability of novolak based negative resists by fluorine plasma treatment. Microelectron Eng 86:769–772

Bolhuis S, van Kan JA, Watt F (2009) Enhancement of proton beam writing in PMMA through optimization of the development procedure. Nucl Instrum Method B 267:2302–2305

Chabinyc ML, Chiu DT, Cooper McDonald J, Strook AD, Christian JF, Karger AM, Whitesides GM (2001) An integrated fluorescence detection system in poly (dimethylsiloxane) for microfluidic applications. Anal Chem 73:4491–4498

Chin G (2003) Highlights of the recent literature: applied physics: Accelerating Lithography. Science 301:1291–1292

Cisne RLC, Vasconcelos TF, Parteli EJR, Andrade JS (2011) Particle transport in flow through a ratchet-like channel. Microfluid Nanofluid 10:543–550

De Marco C, Mele E, Camposeo A, Stabile R, Cingolani R, Pisignano D (2008) Organic light-emitting nanofibers by solvent-resistant nanofluidics. Adv Mater 20:4158–4162

Erickson D, Mandal S, Yang AHJ, Cordovez B (2008) Nanobiosensors: optofluidic, electrical and mechanical approaches to biomolecular detection at the nanoscale. Microfluid Nanofluid 4:33–52

Ertas D (1998) Lateral separation of macromolecules and polyelectrolytes in microlithographic arrays. Phys Rev Lett 80:1548–1551

Grime GW, Watt F (1984) "Beam optics of quardupole probe forming systems". Adam Hilger, Bristol, p 263

Hagen CW, Fokkema E, Kruit P (2008) Brightness measurements of a gallium liquid metal ion source. J Vac Sci Tech B 26:2091–2096

Huang LR, Cox EC, Austin RH, Sturm JC (2003) Tilted brownian ratchet for DNA analysis. Anal Chem 75:6963–6967

Huang LR, Cox EC, Austin RH, Sturm JC (2004) Continuous particle separation through deterministic lateral displacement. Science 304:987–990

Lei Zhang, Fuxing Gu, Limin Tong, Xuefeng Yin (2008) Simple and cost-effective fabrication of two-dimensional plastic nanochannels from silica nanowire templates. Microfluid Nanofluid, 5:727–732

Liu NN, Shao PG, Kulkarni SR, Zhao J, van Kan JA (2010) Nickel injection mould fabrication via proton beam writing and UV lithography. Key Eng Mater 447–448:188–192

Makohliso SA, Giovangrandi L, Léonard D, Mathieu HJ, Ilegems M, Aebischer P (1998) Application of Teflon-AF® thin films for bio-patterning of neural cell adhesion. Biosens Bioelectron 13:1227–1235

Menzel F, Spemann D, Petriconi S, Lenzner J, Butz T (2007) Proton beam writing of submicrometer structures at LIPSION. Nucl Instrum Method B 260:419–425

Moak CD, Reese H, Good WM (1951) Design and operation of a radio-frequency ion source for particle accelerators. Nucleonics 9:18–23

Ottesen EA, Hong JW, Quake SR, Leadbetter JR (2006) Microfluidic digital PCR enables multigene analysis of individual environmental bacteria. Science 314:1464–1467

Phillips KS, Cheng Q (2005) Microfluidic immunoassay for bacterial toxins with supported phospholipid bilayer membranes on poly(dimethylsiloxane). Anal Chem 77:327–334 Private communications

Rolland JP, Hagberg EC, Denison GM, Carter KR, De Simone JM (2004) High-resolution soft lithography: enabling materials for nanotechnologies. Angew Chem 43:5796–5799

Song S, Lee KY (2006) Polymers for microfluidic chips. Macromol Res 14:121–128

Swanson LW, Schwind GA (2008) Charge Particle Optics, 2 edn, 1

Szymanski R, Jamieson DN (1997) Ion source brightness and nuclear microprobe applications. Nucl Instrum Method B 130:80–85

Thorsen T, Maerkl SJ, Quake SR (2002) Microfluidic large-scale integration. Science 298:580–584

Udalagama CNB, Bettiol AA, Watt F (2007) A Monte Carlo study of the extent of proximity effects in e-beam and p-beam writing of PMMA. Nucl Instrum Method B 260:384–389

Udalagama C, Bettiol AA, Watt F (2009) Stocastic spatial energy deposition profiles for MeV protons and keV electrons. Phys Rev B, 80:224107-1–224107-8

van Kan JA, Sum TC, Osipowicz T, Watt F (2000) Sub 100 nm proton beam micromachining: Theoretical calculations on resolution limits. Nucl Instrum Method B 161:366–370

van Kan JA, Bettiol AA, Watt F (2003a) Three-dimensional nanolithography using proton beam writing. Appl Phys Lett 83:1629–1631

van Kan JA, Bettiol AA, Watt F (2003b) Proton beam nanomachining: end station design and testing. Mat Res Soc Symp Proc 777:T2.1.1–T2.1.10

van Kan JA, Bettiol AA, Watt F (2006) Proton beam writing of three-dimensional nanostructures in hydrogen silsesquioxane. Nano lett 6:579–582

van Kan JA, Bettiol AA, Chiam SY, Saifullah MSM, Subramanian KRV, Welland ME, Watt F (2007) New resists for proton beam writing. Nucl Instrum Method B 260:460–463

van Kan JA, Malar P, Armin Baysic de Vera, Xiao Chen, Bettiol AA, Watt F (2011) Proton beam writing nanoprobe facility design and first test results, Nucl Instrum Method A 645:113–115

Watt F, van Kan JA, Rajta I, Bettiol AA, Choo TF, Breese MBH, Osipowicz T (2003) The national university of singapore high energy ion nano probe facility performance tests. Nucl Instrum Method B 210:14–20

Watt F, Bettiol AA, van Kan JA, Teo EJ, Breese MBH (2005) Ion beam lithography and nano-fabrication: a review. Int J Nanosci 4:269–286

Watt F, Breese MBH, Bettiol AA, van Kan JA (2007) Proton beam writing. Mater today 10:20–29

Watt F, Xiao Chen, Armin Baysic De Vera, Udalagama CCN, Ren Minqin, van Kan JA, Bettiol AA (2011) The Singapore high resolution single cell imaging facility. Nucl Instrum Method B. doi: 10.1016/j.nimb.2011.02.028

Whitesides GM (2006) The origins and the future of microfluidics. Nature 442:368–373

Whitlow HJ, Ng ML, Aŭzelyté V, Maximov I, Montelius L, van Kan JA, Bettiol AA, Watt F (2004) Lithography of high spatial density biosensor structures with sub-100 nm spacing by

megaelectronvolt proton beam writing with minimal proximity effect. Nanotechnology 15:223–226

Xianqiao Hu, Qiaohong He, Xiangbo Zhang, Hengwu Chen (2011) Fabrication of fluidic chips with 1-D nanochannels on PMMA substrates by photoresist-free UV-lithography and UV-assisted low-temperature bonding. Microfluid Nanofluid 10:1223–1232

Yager P, Edwards T, Fu E, Helton K, Nelson K, Tam MR, Weigl BH (2006) Microfluidic diagnostic technologies for global public health. Nature 442:412–418

Yea KH, Lee S, Choo J, Oh CH, Lee S (2006) Fast and sensitive analysis of DNA hybridization in a PDMS micro-fluidic channel using fluorescence resonance energy transfer. Chem Commun 14:1509–1511

Zhang C, Zhang F, van Kan JA, van der Maarel JRC ((2008)) Effects of electrostatic screening on the conformation of single DNA molecules confined in a nanochannel. J Chem Phys 128:225109-1–225109-10

Zhang F, van Kan JA, Chiam SY, Watt F (2007) Fabrication of free standing resolution standards using proton beam writing. Nucl Instrum Method B 260:474–478

Zhang C, Shao PG, van Kan JA, van der Maarel JRC (2009) Macromolecular crowding induced elongation and compaction of single DNA molecules confined in a nanochannel. Proc Natl Acad Sci USA 106:16651–16656